J Appl Electrochem (2008) 38:1763–1769
DOI 10.1007/s10800-008-9630-3

ORIGINAL PAPER

Response surface analysis to evaluate the influence of deposition parameters on the electrodeposition of Cu–Co alloys in citrate medium

F. L. G. Silva · J. R. Garcia · V. G. M. Cruz ·
A. S. Luna · D. C. B. Lago · L. F. Senna

Received: 22 January 2008 / Accepted: 26 June 2008 / Published online: 18 July 2008

Abstract Copper–cobalt alloy coatings were deposited on mild steel substrates using sodium citrate electrolytes at room temperature and under direct current. A set of cathodic polarization curves was plotted by varying the mechanical stirring speed of the solution (0–400 rpm), using a range of current densities during the electrodeposition experiments. Factorial design was used to verify the influence of these deposition parameters on the cathodic efficiency, the copper and cobalt content in the coating, the corrosion current density of the coating/substrate system, and the efficiency of the coating in protecting the substrate. The electroplating experiments showed that, with the studied bath composition, high stirring speed and low current density lead to greater cathodic current efficiency and copper-rich coatings. On the other hand, high current density and low stirring speed yields coatings with high cobalt content and a lower cathodic efficiency. Our results show that the studied parameters affect the corrosion current density and the coating efficiency of the coating/substrate system in opposite ways. The best results were obtained increasing the current density and decreasing the mechanical stirring speed. Additionally, three samples were produced in selected deposition conditions. The coatings morphologies were compact, and their grain sizes seemed to enlarge with increasing stirring speed and decreasing current density.

Keywords Electroplating · Copper · Cobalt · Response surface methodology

1 Introduction

Metallic coatings are generally applied to a substrate surface in order to produce coating/substrate systems with enhanced properties. Cu–Co alloys deposited on copper, platinum or silicon substrates are of great interest due to their possible use in data storage systems and sensor technology [1–3]. These applications are based on the giant magneto resistance property of these alloys, meaning that their electrical resistance can be made to vary widely in response to an external magnetic field. This property can only be observed in a metastable solid solution containing few amounts of cobalt in a copper matrix, which enhances the segregation of small Co precipitates, and leads to the formation of a granular alloy. Nonetheless, Cu–Co alloy coatings with high cobalt content and produced on other substrates can also find suitable applications, mainly for catalytic purposes [4–6] and anticorrosive coatings [7, 8].

Several deposition processes have been studied to produce Cu–Co alloys. The physical vapor deposition (PVD) and chemical vapor deposition (CVD) methods are the most frequently used. A simpler and less expensive alternative to obtain Cu–Co alloy coatings involves electrodeposition [4, 9, 10]. However, electrodeposition of metal alloy coatings is a complex process. It requires the control of several chemical and operational parameters, which are, in practice, often chosen empirically and the alloy is then produced at these “optimum conditions”. Therefore, to ensure greater reproducibility and quality, it is important to develop a more scientific approach leading to a better understanding of the alloy deposition

---

F. L. G. Silva · J. R. Garcia · V. G. M. Cruz ·
A. S. Luna · D. C. B. Lago · L. F. Senna (✉)
Departamento de Química Analítica, Instituto de Química,
Universidade do Estado do Rio de Janeiro, Rua São Francisco
Xavier, 524, Maracana 20559-900, Rio de Janeiro, Brazil
e-mail: lsenna@uerj.br

phenomenon. One way to do this is to use experimental design and statistical techniques [11–13] which would allow improvements both in process performance and reliability, leading to the creation of new alloys systems that fulfill industrial needs.

In this work, Cu–Co alloy coatings were produced on mild steel substrates from citrate electrolyte. Experimental design procedures were used to evaluate the effects of deposition parameters such as current density and mechanical stirring speed on the cathodic current efficiency, alloy coating composition, corrosion current density, and the efficiency of the coating in protecting the substrate. The aim of this study was to contribute to a better insight on Cu–Co electrodeposition from citrate electrolytes in order to improve control over the properties of alloy coatings produced with this technology.

2 Experimental methodology

2.1 Cathodic polarization curves

Cathodic polarization curves were galvanostatically obtained in the current density range of 0.13–267 A m^{-2}. AISI 1028 mild steel discs (exposed area of 1.70×10^{-4} m^2) were used as working electrodes, while a platinum net acted as counter electrode. The reference electrode was a saturated mercury (I) sulfate electrode (Hg/Hg_2SO_4), SSE. The experiments were carried out under room temperature, and stirring speed was varied from 0 to 400 rpm. Table 1 describes the chemical composition, pH and conductivity of the bath used in this work. This bath composition was chosen based on earlier studies using similar copper-alloy baths [11].

2.2 Alloy electrodeposition experiments

In order to improve the alloy electrodeposition process and attain a high corrosion current density, an experimental central composite design 2^2 with central axial points was employed [14]. A quadratic model was applied to quantitatively evaluate and describe the response surfaces concerning the effects of current density (I) and mechanical stirring speed (S) on the cathodic efficiency (Ef), the alloy chemical composition (% m/m Cu and % m/m Co), the corrosion current density (I_{corr}), and the coating efficiency (Ef_{coat}) (Table 2). These assays were performed using the same system earlier mentioned, except that mild steel disks (5.31×10^{-4} m^2 of exposed area) were used as the work electrode. The cathodic current efficiency was obtained gravimetrically. The produced layers were dissolved in 20% (v/v) HNO_3 and the alloy composition was determined by inductively coupled plasma optical emission spectrometry (ICP-OES), applying the conditions recommended by the instrument operation manual. Table 2 presents the codified and normal values of the studied variables. A commercial software package (STATISTICA for Windows, release 7.0) was used for the experimental data regression analysis.

Table 1 Chemical composition, pH, and conductivity of the citrate-based electrolyte

Chemical composition (mol L^{-1})			pH	Conductivity (mS cm^{-1})
$CuSO_4$	$CoSO_4$	$Na_3C_5H_6O_7$		
0.02	0.20	1.00	6.76	67.1

Table 2 Central composite design 2^2 experimental matrix, showing codified and normal values of the studied variables

Run no.	Stirring speed (codified values)	Current density (codified values)	Stirring speed (real values) (rpm)	Current density (real values) (A m^{-2})
1	−1	−1	100	5
2	+1	−1	300	5
3	−1	+1	100	15
4	+1	+1	300	15
5	0	0	200	10
6	0	0	200	10
7	0	0	200	10
8	$-\sqrt{2}$	0	58	10
9	0	$\sqrt{2}$	200	17
10	$\sqrt{2}$	0	341	10
11	0	$-\sqrt{2}$	200	3

2.3 Morphological analysis

The influence of deposition parameters on the morphology of the copper–cobalt coatings was analyzed by scanning electron microscopy (SEM).

2.4 Corrosion experiments

The coatings obtained in the solution shown in Table 1 were electrochemically evaluated by potentiostatic polarization curves, using a scan rate of 5 mV s^{-1}. The experiments were performed in a 0.5 mol/L NaCl solution at room temperature. The counter electrode was a platinum net, while the reference electrode was saturated calomel (SCE).

I_{corr} was obtained from the Tafel slopes of the polarization curves, while Ef_{coat} was calculated using Eq. 1:

$$Ef_{coat} = \frac{I_{corr}^{steel} - I_{corr}^{syst}}{I_{corr}^{steel}} \times 100\% \tag{1}$$

where I_{corr}^{steel} is the corrosion current density of the naked steel substrate and I_{corr}^{syst} is the corrosion current density of the coating/substrate system.

3 Results and discussion

3.1 Polarization curves

Figure 1 presents the cathodic polarization curves of the steel electrode in the solution shown in Table 1, over the entire range of mechanical stirring speeds tested. The goals of this assay was to select the current density range for the electrodeposition tests and to verify the effects of both current density and mechanical stirring speed on the cathodic behavior of the solution. In this work, the Cu(II) concentration in the solution was 10-fold lower than the Co(II) concentration. Based on the formation constant (K_f) of both Cu(II) and Co(II) citrate complexes ($K_f^{Cu} = 1.62 \times 10^{14}$ and $K_f^{Co} = 6.76 \times 10^4$, respectively) [15], the stability of Cu(II) citrate complex is higher than that of the Co(II) complex, which decreases the activity of Cu(II) in solution and brings the reduction potentials of both ions closer together. The high concentration of citrate in the medium, however, could permit the formation of cobalt-citrate complexes as well. It means that, in this system, cobalt is probably deposited from both citrate and aquo-complexes.

It is interesting to note that all the polarization curves show frequent changes in slope, which could reflect different deposition mechanisms [16]. At potential values higher than $-1.0\ V_{SSE}$, a straight line is observed, indicating that the deposition process must be kinetically controlled. At lower potentials, all curves present a limit current plateau, probably associated to the Cu(II) ions reduction controlled by diffusion. At potential values more negative than $-1.4\ V_{SSE}$, a new limit current region is observed, probably related to the reduction of Co(II) ions. Similar results have been reported previously [8, 10]. Therefore, it is reasonable to conclude that at potential values less negative than $-1.0\ V_{SSE}$, the coatings are rich in copper, while at potential values more negative than $-1.4\ V_{SSE}$, coatings rich in cobalt can be obtained. Between these values, a range of compositions of Cu–Co alloy coatings can probably be achieved.

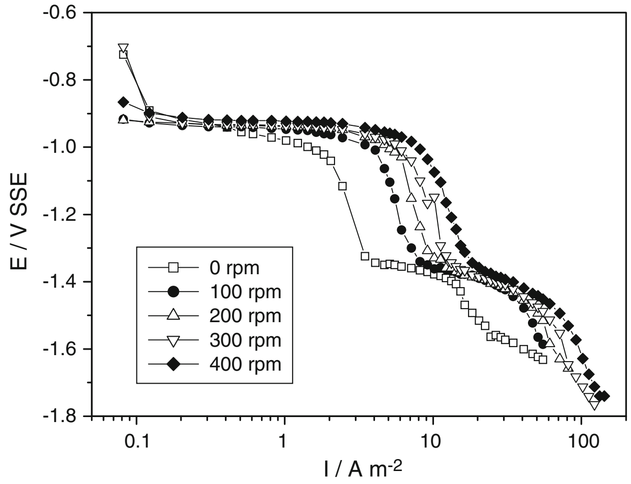

Fig. 1 Galvanostatic polarization curves in the solution described in Table 1

All the polarization curves show a depolarization in response to the increasing of mechanical stirring speed, indicating that this parameter seems to directly influence in the alloy electroplating. The increase of stirring speed enhances the transport of Cu(II) ions to the substrate surface, shifting the limit current regime to higher values of current density. This causes an enlargement in the range of current density controlled by charge transfer. Similar behavior, although to a lesser extent, was observed in Co(II) deposition. Based on these results, a range of current densities and stirring speeds was chosen (Table 2) and the electrodeposition experiments were performed, as described in Sect. 2.2.

3.2 Alloy electrodeposition experiments

The effects of current density and mechanical stirring speed can be better evaluated by applying experimental factorial procedures to the electrodeposition experiments. The complete quadratic surface model between the studied factors and the system response is given by Eq. 2:

$$\hat{y} = b_0 + b_1X_1 + b_2X_2 + b_{11}X_1^2 + b_{22}X_2^2 + b_{12}bX_1X_2 \tag{2}$$

where $\hat{y}$ is the estimated response, X_1 is the current density (I), X_2 represents the stirring speed (S), X_1X_2 is the term of interaction between the current density and the stirring speed (IS), and the b_i are the equation coefficients. Statistical tests ($p = 0.05$) were then used to verify whether the analyzed effects were statistically significant. In the equations presented in this work only the parameters found to affect the system at a level of statistical significance ($p < 0.05$) are shown. It is important to point out that even though some individuals trends could be observed in how I and S influenced the system responses (Ef, % m/m Cu, % m/m Co, I_{corr} and Ef_{coat}), the final results concerning the influence of the studied parameters were obtained using the quadratic response surfaces, which take in account all the responses observed for each effect.

The result model obtained for Ef, estimated from the experiments performed in the bath solution described in Table 1, is represented by the fitted surface response diagram shown in Fig. 2 and defined by Eq. 3. The fitting shows, at a confidence level of 95%, that both I and S

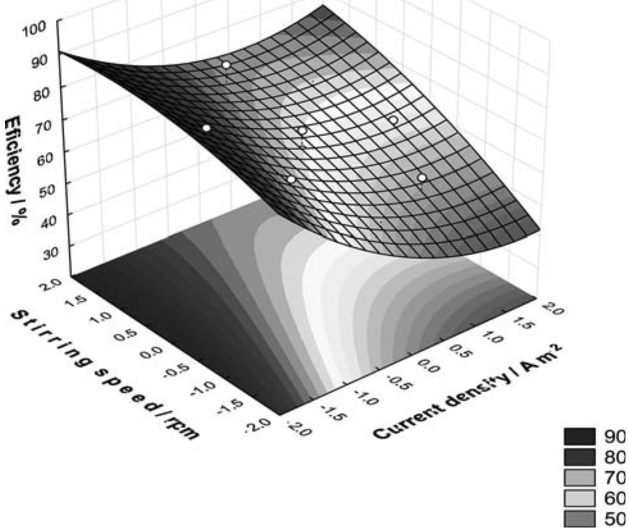

Fig. 2 Fitted surface of standardized effects for cathodic current efficiency

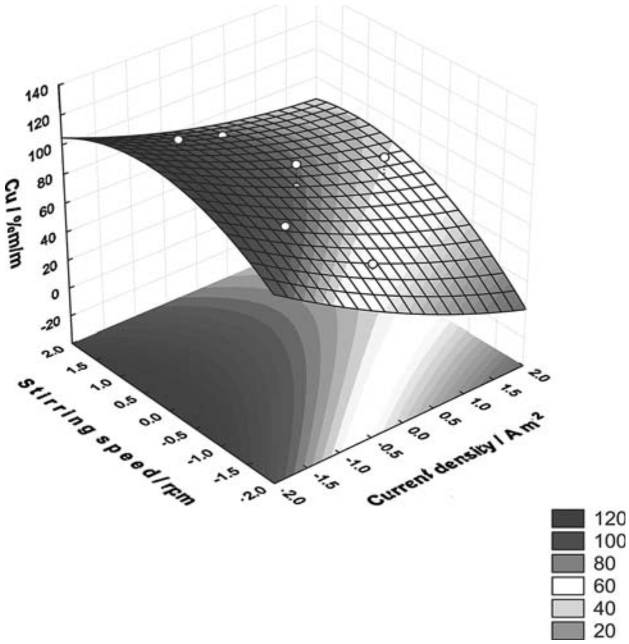

Fig. 3 Fitted surface of standardized effects for % m/m Cu

influence *Ef* in a linear manner ($p < 0.01$ and $p < 0.03$, respectively). It is also interesting to note that the two parameters exert opposing effects on *Ef*, as shown in Eq. 3. This means that high values of current efficiency can be obtained by applying low values of *I* and high values of *S*.

$$\hat{Ef} = 66 - 6.8I + 5.4S \tag{3}$$

Figure 3 and Eq. 4 show the effects of the two deposition parameters on % m/m Cu in the produced alloy. It can be observed that *I* exerts a statistically significant and negative influence on the amount of copper deposited on the substrate ($p < 0.009$). Since copper is the nobler metal in the alloy, its ions are usually easily reduced, and this is probably the main reaction observed at low values of current density. However, at higher current densities, other reduction reactions can take place in parallel, such as the reduction of cobalt or hydrogen ions, which decrease the amount of copper in the coating.

On the other hand, *S* exerts a positive effect on copper deposition, even though the *t* test indicates a borderline *p*-value ($p = 0.05$). It is widely known that stirring enhances the transport of metal ions through forced convection, and this probably helps to increase the copper content in the coating, since it is the nobler element in the alloy. Additionally, the mechanisms proposed to describe copper deposition in citrate medium [17, 18], taking in account pH variation and citrate concentration, suggest that several Cu-citrate complexes can be reduced directly on the electrode surface without prior dissociation. After reduction, the resulting species can be either incorporated directly into the deposit or they can undergo decomplexation, yielding molecules of free complexing agent. Therefore, an increase in the stirring speed may enhance the transport of any free ligand from the electrode surface to the bulk solution after the discharge. These results agree with the polarization curves (Fig. 1), suggesting that copper-rich coatings can be probably obtained at low values of *I* and high values of *S*.

$$\hat{Cu} = 82 - 16I + 10S \tag{4}$$

Concerning the cobalt content in the coating, Fig. 4 shows that *I* exerts a linear, positive, and statistically

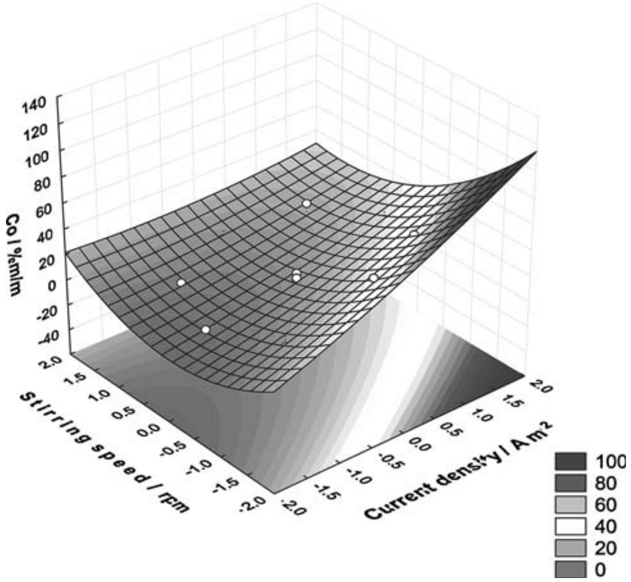

Fig. 4 Fitted surfaces of standardized effects for % m/m Co

significant effect on % m/m Co ($p < 0.003$), in agreement to what was proposed in Fig. 1. This behavior was expected, since increasing the current density favors the deposition of the less noble metal in the alloy, cobalt. On the other hand, the statistically significant effect of S on this variable was linear and negative ($p < 0.007$), as well as quadratic and positive ($p < 0.04$). Comparing the two p-values, it can be seen that the linear and negative effect predominates on % m/m Co. As seen earlier in this work, forced convection may improve copper deposition, decreasing the cobalt content in the coating. Ferreira et al. [11] observed similar results with Cu–Zn alloys produced in a citrate bath. In the present work, however, a depolarization occurred at high current densities (where cobalt deposition is preferred), and high stirring speeds, an effect that may be related to the quadratic term. Equation 5 shows the resulting model for this variable.

$$\hat{\mathrm{Co}} = 11 + 13I - 10S + 7.6S^2 \tag{5}$$

Cu–Co coatings were also produced in the conditions determined by Table 2 and the corrosion of the coating/substrate system was then evaluated as I_{corr} and Ef_{coat}. Equation 6 shows that I influences I_{corr} in a negative and linear manner ($p < 0.04$), whereas S affects the studied variable in a positive and quadratic way ($p < 0.02$). Therefore, I_{corr} tends to decrease linearly with I and increase quadratically with S, which means that coatings with satisfactory anticorrosive performance may be obtained at high current densities and low stirring speeds. These conditions coincide with those where high values of % m/m Co are obtained. Consistent with these findings, El-Rehim et al. [8] reported that Cu–Co coatings with high % m/m Co in the alloy would present better anticorrosion performance. However, the statistical evaluation also shows a positive interaction between both studied parameters ($p < 0.03$), which implies that a simultaneous variation of both I and S in the same direction would increase I_{corr}, limiting the above mentioned conditions. Figure 5 supports the p-values for the estimated effects.

$$\hat{I}_{corr} = 0.10 - 0.03I + 0.06S^2 + 0.06IS \tag{6}$$

As can be seen in Eq. 7, there is an opposite influence of the studied deposition parameters on Ef_{coat}, when compared to the I_{corr} results. Thus, I exerts a linear and positive effect on Ef_{coat} ($p < 0.04$), while S exerts a negative and quadratic influence ($p < 0.02$), as do both parameters together ($p < 0.03$). It means that high I and low S values should favor the production of protective anticorrosion coatings. However, the simultaneous variation of both parameters in the same direction would result in coatings with low protective quality, as shown in Fig. 6.

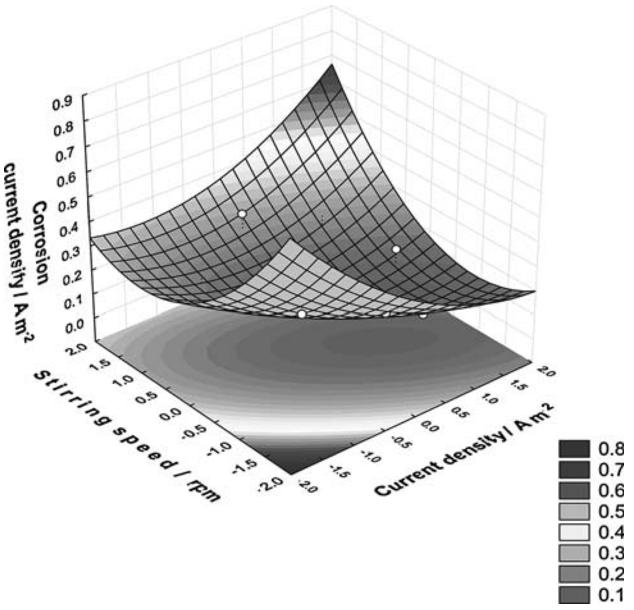

Fig. 5 Fitted surfaces of standardized effects for corrosion current density of the coating/substrate system

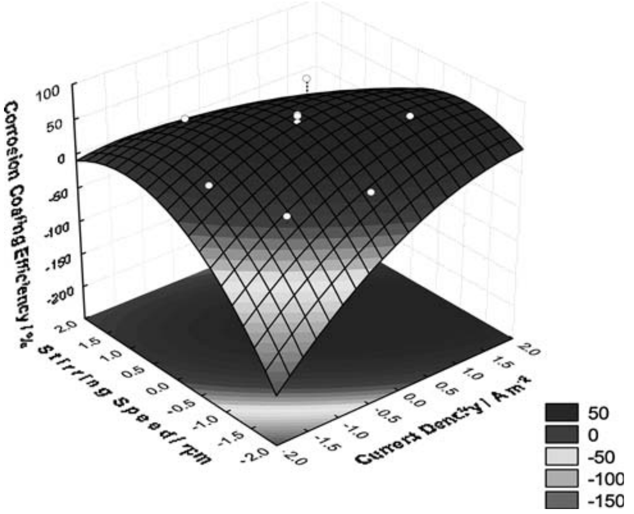

Fig. 6 Fitted surfaces of standardized effects for coating efficiency of the coating/substrate system

$$\hat{Ef}_{coat} = 65 + 12I - 22S^2 - 20IS \tag{7}$$

Based on these results, we selected three conditions (Table 3) for producing the coatings, which were then characterized, in order to correlate their morphological and electrochemical features to the variables studied in this work.

The theoretical and experimental results concerning the values of Ef, % m/m Cu, % m/m Co, I_{corr}, and Ef_{coat}, as well as the open circuit potential (OCP), are shown in Table 3. The theoretical results were obtained by substituting the codified values for each selected condition in the

Table 3 Selected conditions to produce Cu–Co coatings in citrate baths: theoretical an experimental results

Sample	Codified values		Current density (A m^{-2})	Stirring speed (rpm)	Theoretical responses					Experimental responses				
	X_1	X_2			*Ef* (%)	Cu (% m/m)	Co (% m/m)	I_{corr} (A m^{-2})	Ef_{coat} (%)	*Ef* (%)	Cu (% m/m)	Co (% m/m)	I_{corr} (A m^{-2})	Ef_{coat} (%)
A	1	−1	15	100	54	56	42	0.07	70	57	40	48	0.08	73
B	1	1	15	300	65	76	22	0.19	34	64	67	24	0.15	50
C	0	0	0	200	66	82	11	0.10	64	66	82	11	0.10	67

respective variable equations. It can be noted that Sample A, produced with high *I* and small *S* values, shows a % m/m Co greater than % m/m Cu and a low *Ef*, which agrees with the results presented earlier (Fig. 4 and Eq. 5). The coating microstructure was homogeneous and composed of very small and compact grains, with few aggregates on the surface (Fig. 7a), which disagrees with the findings of El-Rehim et al. [8] that coatings with high amounts of cobalt display a rough microstructure with large grain sizes. The coating microstructure seems to be also related to the amount of citrate in the solution, as shown by Gomez et al. [10], as well as to the deposition conditions (*I* and *S*). The I_{corr} and Ef_{coat} values are 0.08 A m^{-2} and 73%, respectively, showing a decrease in the $I_{corr,}$ when compared to naked mild steel AISI 1028 (0.30 A m^{-2}). The OCP value was more negative than that of the naked mild steel (−0.720 and −0.580 V_{SCE}, respectively). Based on these results, this layer is likely to act as a sacrificial coating.

Sample B was obtained at high *S* values and at the same *I* as for Sample A. As shown elsewhere in this work, both *Ef* and % m/m Cu tend to increase with *S*, while % m/m Co decreases with this parameter. Compared to Sample A, Sample B presents higher *Ef* and % m/m Cu values, and smaller % m/m Co result (Table 3). In addition, the microstructure of Sample B was less homogeneous and its grain size, though small, is higher than that of Sample A, which probably reflects an effect of *S* on grain size (Fig. 7b). Therefore, the solution stirring seems to favor growth of nuclei and to disfavor the nucleation process [19]. The I_{corr} and Ef_{coat} values under these conditions are 0.15 A m^{-2} and 50%, respectively, which are less desirable than the results obtained for Sample A, although Sample B does show a lower corrosion current density than naked mild steel AISI 1028. The OCP value was less negative than for naked mild steel (−0.520 V_{SCE}), indicating that Sample B is probably a protective coating.

Using intermediate values for *I* and *S* produces a coating (Sample C), with a coarse, though compact morphology, and large grain sizes (Fig. 7c). The value of *S* is greater than that used for Sample A, which together with the lower *I* probably causes this change in morphology. This joint effect may favor the growth of nuclei and also enhance Cu(II) transport toward the electrode. These results are corroborated by the high % m/m Cu and low % m/m Co obtained. The I_{corr} and Ef_{coat} values are 0.10 A m^{-2} and 67%, which is an intermediate result, comparing to Samples A and B. The OCP value was near that obtained for naked mild steel (−0.610 V_{SCE}).

4 Conclusion

Citrate baths are stable enough and can be used for electrodeposition of Cu–Co alloy to produce shiny coatings. The polarization curves have shown that copper-rich coatings could be produced at potentials less negative than −1.0 V_{SSE}, while layers with a high cobalt content could be obtained at potentials more negative than −1.4 V_{SSE}. On the other hand, depolarization was observed with increasing mechanical stirring speed.

The influence of the deposition parameters *I* and *S* on the studied variables was better understood thanks to statistical treatment. This analysis showed that *Ef* tends to increase directly with *S* and inversely with *I*. Copper-rich layers can be obtained at low *I* values and high *S* values, although the influence of this last parameter was less significant. Adherent and shiny reddish coatings were obtained under these conditions. On the other hand, high *I* and low *S* values yield cobalt-rich, adherent, shiny, and dark gray coatings. A quadratic effect of *S* on % m/m Co was also observed, which probably corroborates the small depolarization noted at potentials more negative than −1.4 V_{SSE}.

The deposition parameter studied here affected I_{corr} and Ef_{coat} inversely, indicating that coatings with good anticorrosive performance can be obtained under conditions of high *I* and low *S* values. However, adjusting both deposition parameters simultaneously in the same direction produces coatings with low protective quality.

The experimental values of the variables studied under the conditions of this work agreed with those predicted by the statistical model. The coatings produced at these conditions show small grains at low *S* values. Increasing *S* and

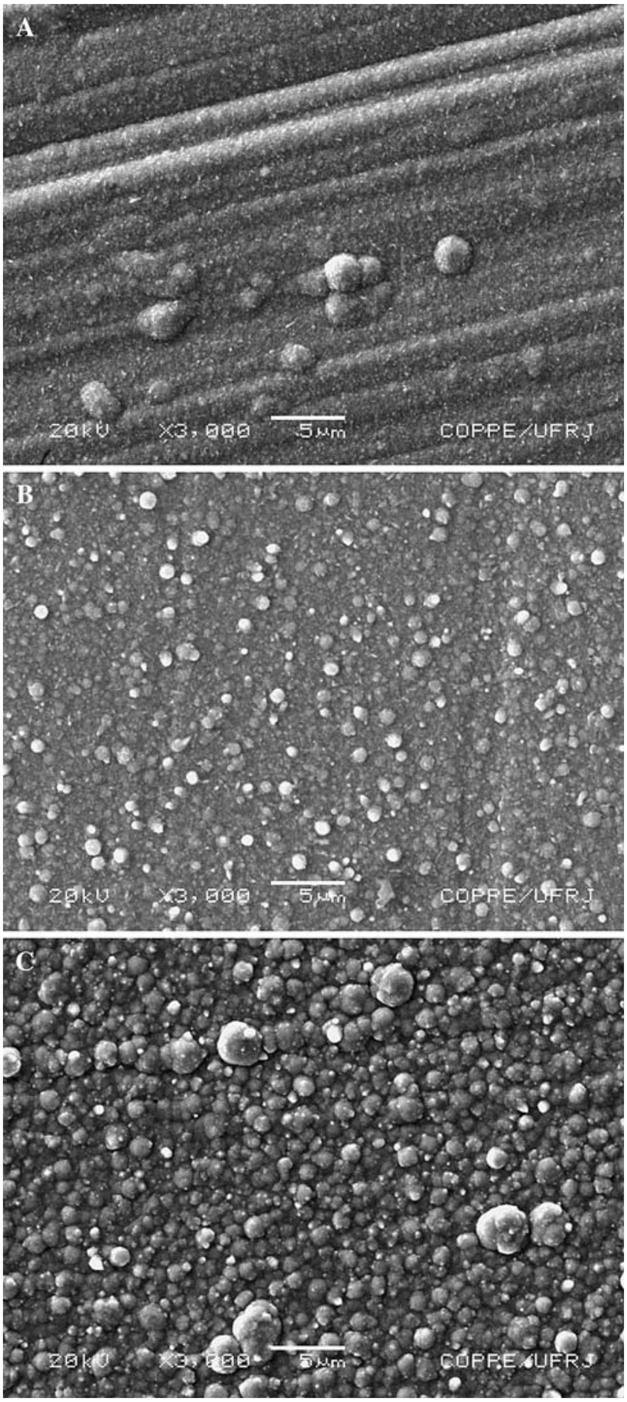

Fig. 7 Morphologies obtained using select deposition conditions: (**a**) 15 A m^{-2}, 100 rpm; (**b**) 15 A m^{-2}, 300 rpm; (**c**) 10 A m^{-2}, 200 rpm

decreasing *I* produce layers with coarse, though still compact, grains. The OCP values were also affected by *I* and *S*, resulting in sacrificial or protecting coatings.

Acknowledgments The authors would like to thank FAPERJ, CNPq, and UERJ for financial support.

References

1. Hyams TC, Kaplan WD, Aurbach D et al (2003) J Electrochem Soc 150:C28
2. Jyoko Y, Kashiwabara S, Hayashi Y (1997) J Electrochem Soc 144:L193
3. Jyoko Y, Kashiwabara S, Hayashi Y (1997) J Electrochem Soc 144:L5
4. Mohamed AE, Rashwan SM, Abdel-Wahaab SM et al (2003) J Appl Electrochem 33:1085
5. Endoh E, Otouma T, Morimoto T et al (1987) Int J Hyd Energy 12:473
6. Vermeiren P, Leysen R, Vandenborre H (1985) Electrochim Acta 30:1253
7. Crousier J, Bimaghra I (1993) J Appl Electrochem 23:775
8. El-Rehim SSA, El-Wahab SMA, Rashwan SM et al (2000) J Chem Technol Biotechnol 75:237
9. Antón RL, Fdez-Gubieda ML, García-Arribas A et al (2002) Mater Sci Eng A 335:94
10. Gómez E, Llorente A, Alcobe X et al (2004) J Solid State Electrochem 8:82
11. Ferreira FBA, Silva FLG, Luna AS et al (2007) J Appl Electrochem 37:473
12. Santana RAC, Prasad S, Campos ARN et al (2006) J Appl Electrochem 36:105
13. San Martín V, Sanllorente S, Palmero S (1998) Electrochim Acta 44:579
14. Neto BB, Scarminio IS, Bruns RE (2001) Como fazer experimentos. UNICAMP, Campinas
15. Lurie Ju (1978) Handbook of analytical chemistry. Mir Publishers, Moscow
16. Greef R, Peat R, Peter LM et al (1985) Instrumental methods in electrochemistry. Ellis Horwood Limited, London
17. Chassaing E, Quang KVu, Wiart R (1986) J Appl Electrochem 16:591
18. Rode S, Henninot C, Vallières C et al (2004) J Electrochem Soc 151:C405
19. Gómez E, Llorente A, Vallés E (2000) J Electroanal Chem 495:19